Sentinel-1 for Observing Forests in the Tropics - SOFT

Final Report - April 2021

Project Name	Sentinel-1 for Observing Forests in the Tropics - SOFT
Contract Number	4000129739/20/I-DT EO Science for Society EOEP-5 Block-4
Issue Date	22.04.2021
Version	2.0
Author	S. Mermoz, T. Le Toan, A. Bouvet
Document Reference	SOFT_FR_202104_v2.0
Document Type	External

GlobEO
Global Earth Observation

CESBIO

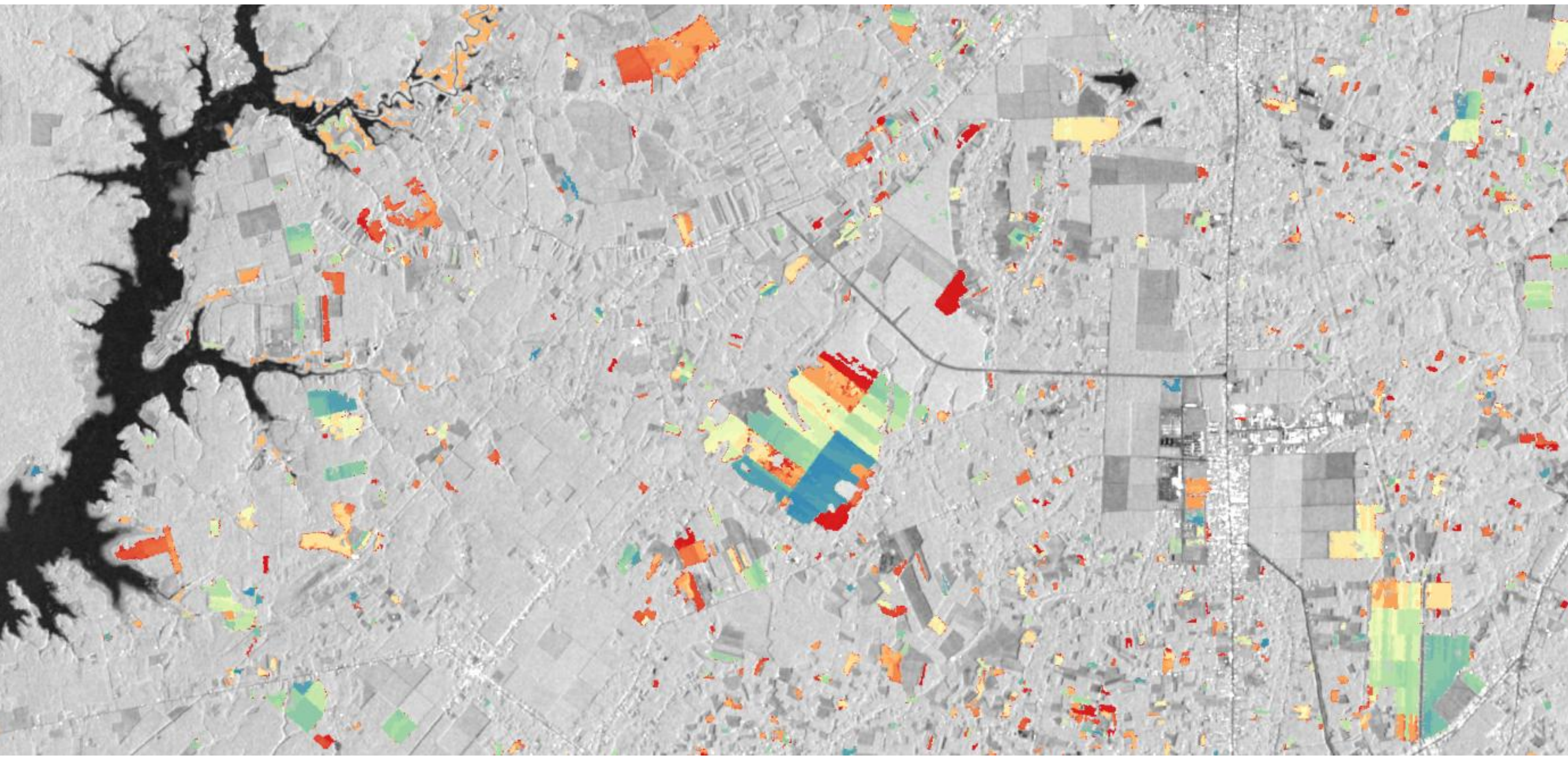

THIS PAGE IS INTENTIONALLY LEFT BLANK

Table of Contents

List of figures

List of tables

List of acronyms

AIL	Action Item List
ARD	Analysis Ready Data
ATBD	Algorithm Theoretical Basis Document
C3S	Copernicus Climate Change Service
CEOS	Committee on Earth Observation satellites
CESBIO	Centre d'Etudes Spatiales de la Biosphère
CNES	Centre National d'Etudes Spatiales
DBH	Diameter at breast height
EO	Earth Observation
ESA	European Space Agency
FAO	Food and Agriculture Organisation
FREL	Forest reference emission level
GEDI	Global Ecosystem Dynamics Investigation
GFW	Global Forest Watch
GLAD	Global Land Analysis and Discovery
GlobEO	Global Earth Observation
GSMaP	Global Satellite Mapping of Precipitations
HPC	High performance computing
IDEAM	Instituto de Hidrología, Meteorología y Estudios Ambientales
INPE	Instituto Nacional de Pesquisas Espaciais
JAXA	Japan Aerospace Exploration Agency
JICA	Japan International Cooperation Agency
MINAM	Ministerio del Ambiente
MGRS	Military grid reference system
NRT	Near real-time
PDF	Probability density function
PNCB	Programa Nacional de Conservación de Bosques
PoC	Proof of concept
RCR	Radar change ratio
RADD	Radar for Detecting Deforestation
REDD+	Reducing emissions from deforestation and forest degradation
SAD	Deforestation Alert System
SAR	Synthetic Aperture Radar
SOFT	Sentinel-1 for Observing Forests in the Tropics
TD	True positive detection
UMD	University of Maryland
UNFCCC	United Nations Framework Convention on Climate Change
VHR	Very high resolution
WP	Work package
WWF	World Wide Fund for Nature

1 INTRODUCTION

1.1 Purpose of the document

The final report aims at fully describing the work done in the frame of the SOFT project, including the description of the programme of work, the activities performed and the main results. It provides a complete description of all the work done during the activity and covers the whole scope of the activity.

1.2 Executive Summary Report

The world's forests have undergone substantial changes in the last decades. Deforestation and forest degradation in particular, contribute greatly to these changes. In certain regions and countries, the changes have been more rapid, which is the case in the Greater Mekong sub-region recognized as deforestation hotspot. Effective tools are thus urgently needed to survey Illegal logging operations which cause widespread concern in the region.

Several research and government organizations have developed systems that provide regular updates to the public, principally based on satellite data. However, most monitoring approaches rely predominantly on optical remote sensing. Nevertheless, a major limitation for optical-based near real time applications is the presence of haze in the dry season (caused by fire) and, more importantly, of clouds persistent in the tropics during the wet season. Cloud cover free SAR images have great potential in tropical areas, but have rarely been used for forest loss monitoring compared to optical imagery. Yet, the dense time series of the Sentinel-1 constellation offer a unique opportunity to systematically monitor forests at the global scale. In addition, it has been recently demonstrated that forest losses can be monitored using Sentinel-1 dense time series based on reliable indicators that bypass environmental effects on SAR signals.

In this context, the primary science objective of the SOFT project is to provide near real time forest loss maps over Vietnam, Cambodia and Laos using Sentinel-1 data to the users of public sectors to support their efforts to control logging and log trade.

SAR-based Algorithms of forest loss detection were first adapted and tested over eleven test sites in the frame of the proof-of-concept (PoC) development. The forest loss detection method from Bouvet et al. (2018) was considered as the best potential candidate algorithms for the reasons detailed in the Final Report. Regarding the Sentinel-1 data processing, we used the pre-processing chain developed at CESBIO and CNES as an operational tool for Sentinel-1 GRD data processing. The chain is based on open source libraries and can be used freely. We selected an adapted forest definitions, selected the test sites and reference data for the PoC, which covered various landscapes and terrain slopes. We also selected relevant ancillary data such as a forest mask, the quality of which has a big impact on the final forest loss detection results. Using these dataset, we deeply analyzed the Sentinel-1 backscatter signal over forest loss and intact forest areas of Vietnam, Cambodia and Laos, which was needed to adapt the forest loss detection method. The quality of maps resulting from the PoC was analysed and assessed qualitatively and quantitatively.

The results of the PoC were extended to the whole Vietnam, Laos and Cambodia for the years 2018 to 2020. We optimized, installed and ran the scripts (in Python) onto the high performance computing (HPC) cluster of the CNES. Then, the processing of the whole study area has been achieved. We mosaicked the resulting maps, checked their quality and manually corrected outliers.
This led to the final map which is the main outcome of the SOFT project. The map provides clear hints of the spatial and temporal distribution of forest losses. For example, the difference between high forest losses currently happening in Northern Laos versus low forest losses in Northern Vietnam is clearly seen, although the whole Northern mountainous region is covered by similar forest types.

We also compared the forest loss surface areas obtained from our method with the results from GFW and GLAD. Although we do not consider the maps of GFW and GLAD as a benchmark and although the use of Sentinel-1 is basically much more relevant in term of timely detection of forest losses, we quantitatively compared the statistics per year and country and qualitatively compared both maps. The results from this study and from GFW are remarkably similar, the largest difference (23%) being found for Laos in 2019. This result highlights the fact that our detection system can be used as an alert system (fast detection from sentinel-1 data) and as an annual detection system similar to GFW, used for example to compute national statistics.

The final map was thoroughly validated following the recommandations from Olofsson (2014 and 2020). We chose as sampling design a stratification with stratas defined by the map classes, mainly to improve the precision of the accuracy and area estimates. We specified a target standard error for overall accuracy of 0.01 and supposed that user's accuracies of the change class is 0.70 for forest disturbances and 0.90 for intact forest. The resulting sample size was therefore n=803 in total, which we have rounded up to 1 000 samples. We then assessed the allocation of the sample to strata so that the sample size allocation results in precise estimates of accuracy and area. We followed Olofsson’s recommendations and allocated a sample size of 100 for the forest disturbance stratum, and then allocated the remainder of the samples to the intact forest classes, i.e. 200 in the buffer areas around detected disturbances, and 700 in intact forest outside of these buffers. We used when possible freely accessible very high spatial resolution imagery online through Google Earth™, which presents low cost interpretation options. When Google Earth images were not available at the relevant dates, we instead accessed Planet’s very high-resolution analysis-ready mosaics as reference data. We then calculated the resulting confusion matrix presented in terms of the sample counts and the confusion matrix populated by estimated proportions of area, used to report accuracy results. The estimated user's accuracy (±95% confidence interval) is 0.95 for forest disturbances and 0.99 for intact forest (including buffer areas around disturbance) and the estimated producer's accuracy is 0.90 for forest disturbances and 0.99 for intact forest. Finally, a quality assessment was performed by comparing the final map to existing optical-based products. The estimated area of 2018 and 2019 deforestation according to the reference data was 23 437 ± 2 140 km².

1.3 Context

Over the last 25 years, the world’s forests have undergone substantial changes. Deforestation and forest degradation in particular contribute greatly to biodiversity loss through habitat destruction, soil erosion, terrestrial water cycle disturbances and anthropogenic CO_2 emissions. Regarding the latter, deforestation and forest degradation accounted for 77% and 13%, respectively, of the total net flux attributable to land use and land cover changes over the period from 1850 to 2015 (estimated to have been 145 ± 16 PgC globally with 102 ± 5.8 PgC in the tropics, according to Houghton and Nassikas, 2017).

In certain regions and countries, the changes have been more rapid, which is the case in the Greater Mekong sub-region recognized as deforestation hotspot, where forest loss from 2009 to 2030 is projected to reach 17% to 34% of the total forest area (15 to 30 million ha) (WWF, 2013). In this region, illegal and unsustainable logging and conversion of forests for agriculture, construction of dams and infrastructure are the direct causes of deforestation and biodiversity loss driven by population growth, increasing market demand, and policies that promote short-term economic growth. Commercial logging and log exports are regulated by governments in all Greater Mekong sub-region countries. However, higher demand and weak law enforcement have hindered efforts to control logging and the log trade. Effective tools are thus urgently needed to survey Illegal logging operations which cause widespread concern in the region.

Vietnam is among the countries with the greatest annual changes in primary forest area and planted forest area in the last 20 years. According to the FAO, the extent of primary forest in Vietnam decreased at rates of 6.94%, 15.6% and 1.21% in 1990 to 2000, 2000 to 2005 and 2005 to 2010, respectively. In 2020, the proportion of primary forets area reaches 0.5% of the total surface area (Table 1). Meanwhile, the extent of planted trees increased with values of 0.75 Mha in 1990, 1.92 Mha in 2000 and 3.08 Mha in 2010. The FAO currently considers Vietnam to be a reforesting country because tree plantations are included as forests in the FRA process, as shown by the forest area temporal evolution from 1990 to 2020 in Table 1. On the contrary, the amount of forest in Cambodia dropped from approximately 11 Mha to 8 Mha between 1990 and 2020. Laos as well experiences a constant decline of its forest surface.

Table 1. Forest area in 1990, 2000, 2010 and 2020, forest area proportion in 2020 and primary forest proportion in 2020 in Vietnam, Cambodia and Laos according to FAO (2020).

	Vietnam	**Cambodia**	**Laos**
Forest area 1990 (ha x 10^3)	9 376	11 005	17 843
Forest area 2000 (ha x 10^3)	11 784	10 781	17 425
Forest area 2010 (ha x 10^3)	13 388	10 589	16 940
Forest area 2020 (ha x 10^3)	14 643	8 068	16 595
Forest area % of land area 2020	47.2	45.7	71.9
Primary forest % of forest area 2020	0.5	4	-

A remote sensing based near real-time (NRT) forest monitoring system with dedicated user needs assessment is adapted to combat deforestation, providing information on newly deforested areas in vast and sometimes inaccessible forests. These systems play a valuable role to :

- Provide early detections of illegal forest loss. System alerts developed in countries like Brazil and Peru have been critical to increasing the capacities of law enforcement and land management agencies in reducing illegal deforestation.
- The detection of active forest loss (hotspots) is important for reducing emissions from deforestation and forest degradation (REDD+) implementation when tracking forest area change that requires immediate response or interventions, although early losses detection is not required in international forest conservation agreements such as REDD+,
- Support national statistical reporting programs,
- Complement a current annual global forest cover loss product, implemented in collaboration with Google and World Resources Institute as part of Global Forest Watch (GFW - Hansen et al., 2013). The annual product is based on a calendar year update, first prototyped using Landsat data from 2000.

At the regional scale, early warning system would help Vietnam to integrate a number of on-going Committee on Earth Observation satellites (CEOS) activities and data in support of forest monitoring for the Mekong Delta region.

1.4 Background

Several research and government organizations have developed systems that provide regular updates to the public, principally based on optical remote sensing data. With a coarse spatial resolution (MODIS data, 250m), the FORMA (Wheeler et al., 2014), Terra-I (Reymondin et al., 2012) and IDEAM systems are developed at the pantropical scale (except IDEAM covering only Colombia) and are respectively available biweekly, monthly and quarterly. DETER-B (Diniz et al., 2015), a Brazilian operational system, provides results with a 60 m spatial resolution and a 5-day frequency. It is developed by the Instituto Nacional de Pesquisas Espaciais (INPE), based on AWiFS data and including a photointerpretation step. Most recently, the Brazilian SAD (Deforestation Alert System; civil society) alerts were further innovated by incorporating Sentinel imagery, both optical and radar. Finally, with the medium resolution of 30 m Landsat data, the MINAM (Peru) and the University of Maryland (UMD) produce forest alerts dataset every week: PNCB Early Warning Alerts, and Global Land Analysis and Discovery (GLAD) forest alerts (Hansen et al., 2016) respectively.

A NRT forest loss monitoring protocol starts with forest losses detection as precisely and quickly as possible. That's why medium-resolution Landsat and Sentinel-based alerts have replaced coarse-resolution (MODIS)-based alerts as the standard. Thereby, the detection of large areas (> 3 ha) is now well controlled globally. In less than a decade, sensing capability for automated forest-loss alerts has improved resolution from 1 km to 10 m. Such operational forest alerts systems should allow states or forest managers to fight against drivers of deforestation, which are generally linked to illegal activities. They can also be used for protected areas management, community forest monitoring, management of agricultural and other productive concessions and raising awareness (Finer et al., 2018).

However, most monitoring approaches rely predominantly on optical remote sensing, due to the opening of the Landsat archive in 2008 together with the availability of easily downloadable fully processed images. Hansen et al. (2016) demonstrated the potential and constraints of operational Landsat based forest loss alerts for the humid tropics. Nevertheless, a major limitation for optical-based NRT applications is the presence of haze in the dry season (caused by fire) and, more importantly, of clouds persistent in the tropics during the wet season. In fact, clouds during the wet season may cause important temporal detection delays, which contradicts the need for fast forest loss alerts. In French Guiana for instance, Ballère et al. (2021) found a median temporal delay of 143 days (more than 4.5 months) using the GLAD optical-based system for year-round activities such as gold mining. And some countries like Vietnam suffer from pervasive cloud cover throughout a large part of the year.

Cloud cover free Synthetic Aperture Radar (SAR) images have great potential in tropical areas, but have rarely been used for forest loss monitoring compared to optical imagery (for notable exceptions, refer to Mermoz and Le Toan, 2016; Lohberger et al., 2018; Reiche et al., 2021), partly because of the scarce data availability until the Sentinel-1 program (Reiche et al., 2016). An exception is the JJ-FAST system developed by the JAXA/JICA, based on ALOS-2 radar data that produce forest loss alerts over 77 tropical countries every 1.5 months with a spatial resolution of 5 ha (Watanabe et al., 2017).

The dense time series of the Sentinel-1 constellation offer a unique opportunity to systematically monitor forests at the global scale. Since the launch of Sentinel-1 in 2014, SAR images are now easily accessible with systematic acquisitions at a 5x20 m spatial resolution and a 6- to 12 days revisit time (depending on the location) in all weather conditions. Although the C-band frequency of the Sentinel-1 SAR system is less adapted for forest loss detection than the longer wavelengths (because it may lead to confusion between the intact forest and deforested area due to the backscatter variability of deforested area having a diversity of surface conditions), large-scale forest disturbances maps have emerged very recently, mostly during the SOFT project. Two notable examples are detailed below :

- Doblas et al. (2020) used Google Earth Engine to extract some 8 million samples of Sentinel-1 backscatter data over the Brazilian Amazon, and then tested two different approaches to deforestation detection (adaptive linear thresholding and maximum likelihood classification). The results were evaluated, reaching more than 95% of global accuracy. This research has backed the creation of a fully-automated, cloud-based deforestation detection system, which is actually running at INPE's servers.
- Reiche et al. (2021) released a new forest disturbances alerts detection system based on Sentinel-1 data (RADD). The detection system was built on prior developments and publications (e.g. Reiche et al., 2018). The user's and producer's accuracies of confirmed disturbance alerts were 97.6% and 95.0%, respectively, suggesting confident detection of forest disturbances larger than or equal to 0.2 ha. When including samples representing disturbance events <0.2 ha, the producer's accuracy was 83.5%. Note that validation was performed using probability sampling with three strata and a total of 1100 sample points. This work represents a step forward because of the large study area (Congo Basin and insular South-East Asia so far) and because the map is available via the GFW platform.

It has been therefore demonstrated that forest losses can be monitored using Sentinel-1 dense time series based on reliable indicators that bypass environmental effects on SAR signals. These methods have been successfully applied at the local/regional scale and are now being adapted at the pan-tropical scale.

2 WORK TO BE PERFORMED

This section details the work to be performed in the frame of the SOFT project, including the description of the work packages (WP).

2.1 Scientific and technical objectives

As detailed in the proposal of the SOFT project, the primary science objective is to provide NRT forest loss maps over Vietnam, Cambodia and Laos using Sentinel-1 data to the users of public sectors to support their efforts to control logging and log trade.

The major technical objective is to build on methods developed for mapping forest loss from Sentinel-1 data, identify the weaknesses in these methods when applied in various conditions and where possible address these issues and adapt the methods to apply them at the country scale. The quality of the maps are verified so that they can be used with confidence.

GlobEO and CESBIO had to implement and demonstrate forest monitoring capabilities exploiting to the maximal extent the two Sentinel-1A and 1B platforms. Optical sensors such as Sentinel-2 were not considered because of the frequent cloud cover in these tropical regions. The demonstration covered the following types of applications and scope:
- The regional demonstration covers relevant areas in Vietnam, Cambodia and Laos.
- The temporal coverage of the demonstration ranges from January 2018 to January 2021.
- The demonstration is performed in a NRT scenario.
- Maps are thoroughly validated based on reference data obtained from in situ observations and mainly from very high resolution (VHR) optical images.
- The system has to operate efficiently in a cloud computing environment, e.g. access the EO input data in an efficient and dynamic manner. Code optimization is performed to be able to manage the large quantities of data mandatory for the application.

2.2 Work packages

2.2.1 WP 100: Management

This work package lasted from the beginning of the project. As a reminder, the objectives of the WP were to carry out an effective management of the project and coordinate and control all the work done within the consortium. The tasks are:

- **WP 110 Project management and reporting**
    - Organise, monitor and control all project activities and ensure the overall integrity of all WPs

- Report on the progress of the work on a regular basis to the ESA Technical Officer by providing monthly review reports to the Agency,
- Provide meeting agendas to the Agency, at least 1 week prior to each progress meeting (done by teleconference) and 2 weeks prior to each project review (i.e. Kick-Off, Final Review);
- Write the minutes of all progress meetings and project reviews
- Maintain an up to date Action Items List (AIL)
- Take all steps necessary to maintain the schedule. In case of departure from schedule, the project manager shall notify immediately the ESA Technical Officer and propose corrective actions to recover all scheduling over-run;
- Check and review all project deliverables for quality and completeness before delivery.
- Coordinate the participation of the end-user organisations to the project.

- **WP120 Dissemination**
  - Promote and disseminate the results of the project.

2.2.2 WP 200: Algorithm development

This work package lasted during the first 6 months of the project from March to September 2020. The objectives of the WP were to develop, select and adapt SAR-based algorithms of forest loss detection. The tasks are:

- **WP 210 Technical and scientific engineering**
  - Review of state-of-the-art in SAR-based forest loss detection and selection of candidate algorithms.
  - Test the retained algorithms over a set of 5-10 test sites representative of the variety of configurations (type of forest loss, availability of Sentinel-1).
- **WP 220 Proof-of-Concept development**
  - Converge towards a unique algorithm, or a set of algorithms with application rules, which provide satisfying results over the 5-10 test sites.

2.2.3 WP 300: Large scale mapping

The objectives of this WP were to upscale the results from the PoC to extend it at the regional scale (Vietnam, Cambodia, Laos), and to produce the final forest loss maps. WP 300 started 2 months after the kick-off and lasted until the end of the project. The tasks are:

- **WP 310 Demonstrator implementation**

- Implement the algorithms in a cloud-computing environment
- Produce forest loss maps at a monthly time scale

- **WP 320 Consistency assessment**
  - Check the reliability of the large-scale implementation of the algorithms with respect to the PoC
  - Check the consistency of the results at the regional scale

2.2.4 WP 400: Validation

The objectives of the WP were to carry out a thorough validation of the produced maps. This WP started in October 2020 until the end of the project. The tasks are:

- **WP 410 Demonstrator campaign and analysis**
  - Collect reference data mainly from very high resolution optical images.
  - Carry out a field campaign in Vietnam to collect reference data with Vietnamese partners and analyse the results of the demonstration campaign.
- **WP 420 Accuracy assessment**
  - Accuracy assessment following Olofsson et al. (2014,2020), with reference data from the field and from VHR optical imagery.

3 ACTIVITIES PERFORMED AND RESULTS: WP 100

Project management was smooth, which was facilitated by the small number of partners in the project. Discussions were almost daily and usually related on work planning, technical matters, and human resource recruitment. All project activities were organised and controled to ensure the successful completion of the project.

Reporting consisted in gathering and synthetizing the advancements and results, and writing and delivering to ESA the monthly review reports, the ATBD, the mid-term review report (MTRR), the validation report, the final report and the executive summary report (ESR).

All planned activities were achieved with the following deviations that were reported and detailed in the monthly reports :

- **Negative effects of Covid-19 on the project**
  - The exceptional health situation that started exactly at the beginning of the project has had an impact on the WP 410. No field campaign in Vietnam could be carried out to collect reference data together with Vietnamese partners, because of the travel ban. Our Vietnamese partners were unable to organize any field campaign in 2020. We discussed the possibility to use field data already acquired in 2018 and 2019, but the sampling design was not adapted to our study (very small areas covered compared with our study area, small number of field dat etc.). We finally successfully validated the forest loss maps using VHR optical data.

- France was confined from March 17, 2020 to May 11, 2020 and from October 30, 2020 to December 15, 2020, which made recruiting complicated especially at the beginning of the project. Meanwhile, the contract of Alexandre Bouvet at CESBIO could be renewed from July 2020 to work on the SOFT project.

- **Delivery of the forest disturbances maps**

The maps are being delivered in April 2021, instead of December 2020 due to the processing duration of the data.

Regarding dissemination, a paper summarizing the main results of the projects will be submitted to a scientific journal with peer-review process before July 2021. A review paper gathering the work achieved on forest loss detection using SAR data is also in preparation.
The particular context related to the Covid19 led to the cancelation of numerous workshops and conferences, including Forestsat 2020 that should have taken place in Krakow, Poland, for which it was basically planned to submit a contribution on the SOFT project. Nevertheless, numerous events are being organized online. The SOFT project will thus be presented at the EGU online General Assembly 2021 on Monday, 26 April 2021 in session BG11 - 'Remote sensing for forest applications' - EGU21-16177 : *Forest disturbances detection in Vietnam, Cambodia and Laos using Sentinel-1 data*.

4 ACTIVITIES PERFORMED AND RESULTS: WP 200

4.1 Selection of the forest loss detection method

The team first performed a bibliographic review related to forest disturbances detection using SAR, with Sentinel-1 based studies analyzed first, followed by studies based on C-band data in general and then other frequencies. The results of the bibliographic review have been detailed in the ATBD.

However, the forest loss detection method from Bouvet et al. (2018) was considered as the best potential candidate algorithms for the following reasons :

- CESBIO and GlobEO are convinced of the potential of the method, which provided excellent results over Peru (Bouvet al., 2018), French Guiana (Ballère et al., 2021), Gabon (Hirgschmugl et al., 2020), Brasil and Vietnam (unpublished results).
- CESBIO and GlobEO created this method and thus perfectly know how to improve or adapt it to Vietnam, Cambodia and Laos.
- The short time of the project (1 year) did not allow for a thorough comparison of existing methods. In addition, CESBIO already performed this round review exercise before the SOFT project and results showed that Bouvet’s method provided more accurate maps with lower computation time over selected test sites than others’s methods.

The forest loss detection system that we adopted is composed of two steps:

- Detect shadows that appear or disappear in a series of images, and,
- Reconstruct the deforested patches associated to the shadows.

It is important to note that the main advantage of the method is to avoid false alarms detection, which would be far worse when forest loss patches are detected in a classical manner without the prior detection of shadows. The method is fully described in the ATBD, in Bouvet et al. (2018) and Ballère et al. (2021).

Regarding the Sentinel-1 data processing, we used the pre-processing chain developed at CESBIO (https://gitlab.orfeo-toolbox.org/s1-tiling/s1tiling), as an operational tool for Sentinel-1 GRD data processing and tiling per the 100 km MGRS used by the Sentinel-2 processing system. The chain is based on open source libraries and can be used freely (Inglada and Christophe 2009).

4.2 Forest definitions

According to the reports submitted by Vietnam, Cambodia and Laos to the UNFCCC (respectively the first summary of information for Vietnam, the Cambodia forest report 2016, and the report of the technical assessment of the proposed forest reference emission level - FREL), Vietnam and Cambodia use the same forest definition, i.e. a tree cover of 10%, a minimum tree height of 5 m at maturity and a minimum area of 0.5 ha. Laos employs a tree cover value of 20%, 10 cm stand diameter at breast height (DBH) and 0.5 hectares of area. The plantations such as rubber, oil palm, teak, acacia and eucalyptus and other kinds of trees which fall under the above criteria area also classified as forests.

In this study, we defined forest as at least 5 m tall trees with a tree cover exceeding 50%. Forest loss is defined as a forest area with a tree cover larger than 50% before disturbance and very low after disturbance (less than 10%, although this value is qualitative). In fact, we assumed that forest loss detection methods based on Sentinel-1 backscatter does not allow to identify forest loss over low tree cover areas. In addition, this definition is also used in Hansen et al., (2013), which is crucial when comparing the results from both methods.

4.3 Sites selection for the PoC

We selected 110x110 km^2 MGRS tiles as study sites with natural forests and plantations, flat and steep terrain, and with available very high resolution (VHR) images in Google Earth. Table 2 summarizes the main characteristics of the selected tiles, i.e. :

- Country in which the tile is located,
- Forest proportion in 2017, i.e. the proportion of forest relative to the entire tile without taking into account permanent water, using the tree cover map from Potapov et al. (2019),
- Forest loss from 2000 to 2017, i.e. the proportion of forest loss using the GFW annual product (Hansen et al., 2013), relative to the entire tile without taking into account permanent water,
- Mean slope over forest, i.e. the mean slope value over areas with tree cover higher than 50% in 2017.

Table 2. Main characterictics of the selected tile in the frame of the WP 200, i.e. country in which the tile is located, forest proportion in 2017 relative to the entire tile without taking into account permanent water, proportion of forest loss from 2000 to 2017 relative to the entire tile without taking into account permanent water and mean slope value over areas with tree cover higher than 50% in 2017.

	Country	Forest proportion in 2017 (%)	Forest loss (%)	Mean slope over forest (°)
48PVV	Cambodge	25.1	15.3	3.2
48PWV	Cambodge	52.1	28.5	3.6
48PYA	Cambodge - Vietnam Laos	60.1	21.3	12.1
49PBS	Vietnam	67.2	21.4	16.1
48PZC	Vietnam	58.5	21.1	17.9
48QXD	Vietnam - Laos	72.9	18.8	14.6
48PUT	Cambodge	73.9	12.3	8.8
48PXT	Vietnam - Cambodge	28.5	12.2	3.8
48QVF	Laos - Vietnam	83.6	10.4	20.4
48QTH	Laos	76.2	16.4	21
48QVK	Vietnam	50.6	7.3	23.1

We tested the method over the following 6 tiles : 48PVV, 48PWV, 48PYA, 49PBS, 48PZC and 48QXD (in white in Figure 1), and quantitatively assessed the results over these tiles using reference data described in section 4.4. Among the 6 test tiles, 3 tiles are located mainly in Vietnam and 3 tiles in Cambodia, with 2 tiles intersecting Laos. Five out of the 6 tiles have a forest proportion higher than 50% and all the tiles show a proportion of forest loss higher than 15%. The mean slope value over forest ranges between 3 and 18°. More information related to these tiles is provided in the ATBD.

We then tested the retained method over 5 other tiles : 48PUT, 48PXT, 48QVF, 48QTH and 48QVK (Figure 1). The test was qualitative as no reference data could be selected over these tiles because of the lack of historical VHR optical data (Planet free cloud mosaic data were not released yet before September 2020).

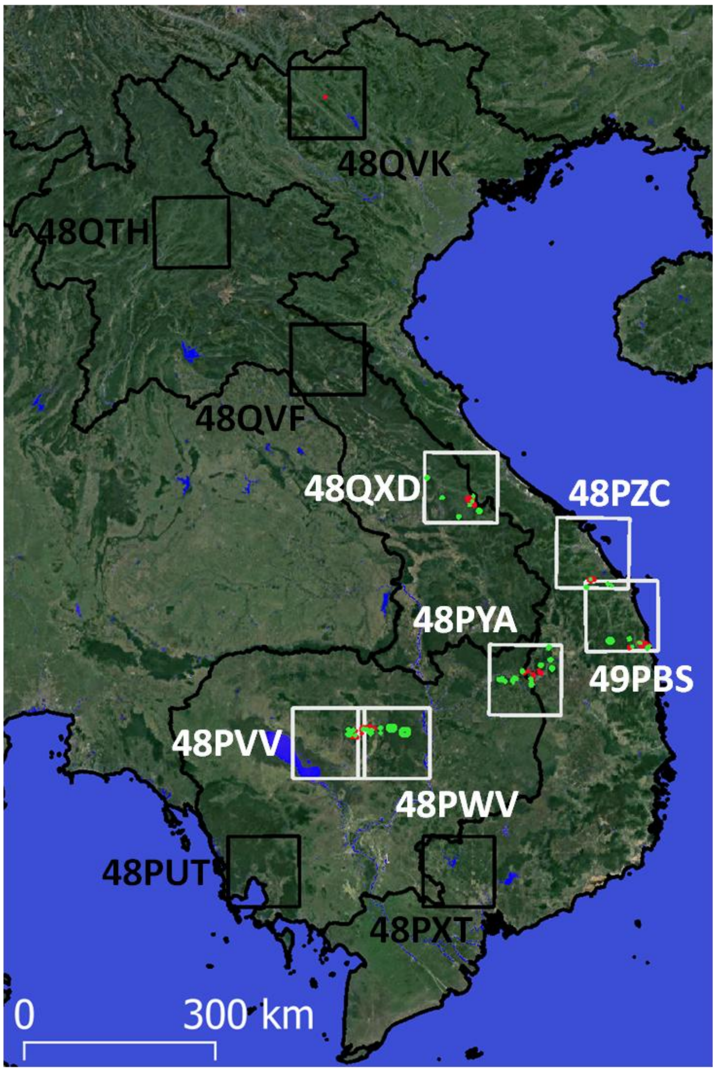

Figure 1. Study sites used in the proof-of-concept development. Reference data (forest loss in red and intact forest in green) were selected in the tiles in white and are described in section 4.4.

4.4 Reference data selection for the PoC

Reference data were selected manually to analyze the temporal backscatter over forest loss and intact forests areas, in order to 1) understand the interactions of the SAR backscatter before forest loss and after forest loss events, and 2) quantify the separability of forest loss areas and intact forest areas in term of detection. We extracted polygons of forest loss and intact forest in test sites through visual interpretation of Google Earth and Sentinel-2 Cloudless images (https://s2maps.eu). At least two available images should be acquired close in time before and after the time window of the PoC, i.e. from end of 2017 to end of 2019. In general, several images from historical data were analysed to ensure reliable selections. The following criteria were used to choose the reference data:

- Selection of forest loss areas in natural forests and plantations,
- Selection of small (< 1 ha) and larger plots,
- Selection of plots over flat and steep terrain,
- Selection of plots over various landscapes, with preferably different drivers of deforestation,
- Only clear-cut areas were extracted.

The spatial distribution of the reference polygons are shown in Figure 1 and the numbers and sizes of the reference polygons are shown in Table 3. A total of 539 plots were selected in 5 sites over 6 MGRS tiles: 48PVV, 48PWV, 48PYA, 49PBS, 48PZC and 48QXD. The histogram of the reference plots size is shown in Figure 2. Approximately 69% of the intact forest reference plots have a surface area lower than 100 ha, and 76% of the forest loss reference plots have a surface area lower than 2 ha.

Table 3. Numbers and sizes of the reference polygons constituting the training and testing database for forest loss assessment.

	Nb. areas	Mean size (ha)	Surface (ha)
Forest loss	457	4.3	1 971
Intact forest	82	381.2	31 260

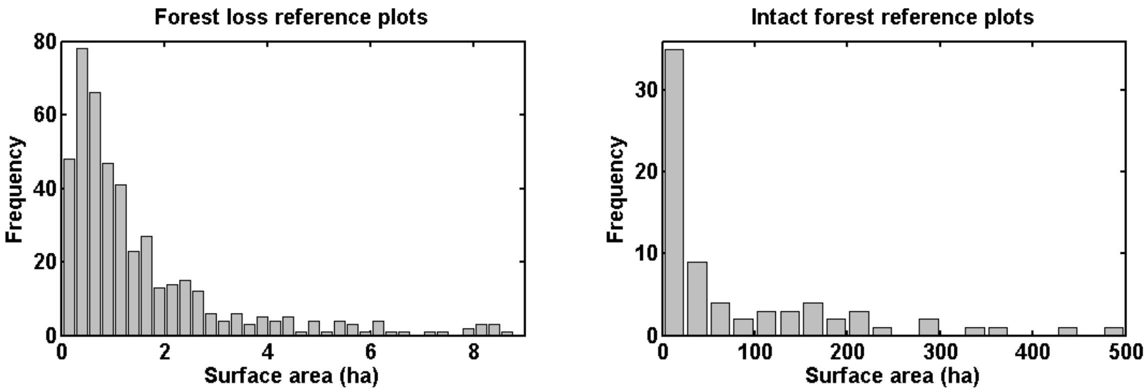

Figure 2. Distribution of the forest loss and intact forest reference plots surface area.

Although no tile has been selected as a study site in the mountains of Northern Vietnam and Laos, the distributions of the terrain slope values over the forest loss and intact forest reference plots (Figure 3) show that reference data have been chosen over a variety of reliefs, with mean values up to 12.5° and 23.5° for forest loss and intact forest plots repectively, over the tile 48PZC for example. The selection of these plots ensures the faisability of the analysis in flat and steep areas detailed in the ATBD. This is crucial as forests over slopes exceeding 20° represent 5.3% of the whole study area and 11.3% of total forest area (Mermoz et al., 2016).

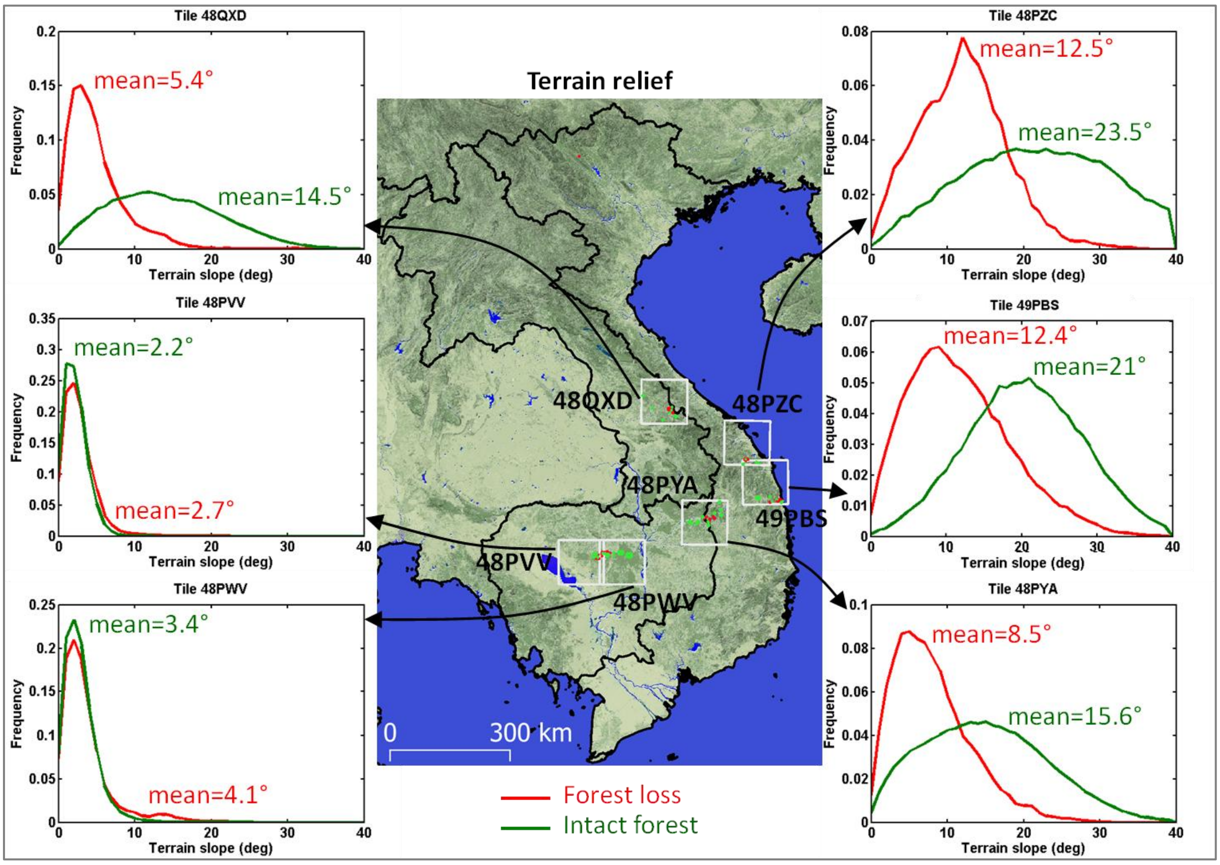

Figure 3. Distribution of the terrain slope values over the forest loss and intact forest reference plots.

4.5 Ancillary data selection

In addition to Sentinel-1 images, numerous ancillary data were used in the project and are summarized in Table 4.

Table 4. Summary of ancillary data

Dataset type	Dataset name	Time frequency	Resolution	Reference
Forest mask	Tree canopy cover	Annual	30m	Potapov et al. 2019
Forest loss	Global Forest Watch	Annual	30m	Hansen et al. 2013
Forest loss alerts	GLAD Alerts	Weekly	30m	Hansen et al. 2016
Forest loss alerts	JJ-Fast	1.5 months	5 ha	Watanabe et al. 2017
Tree canopy height	Tree canopy height	Annual	30m	Potapov et al. 2021
Precipitations	GSMap	Daily	0.1°	Kubota et al. 2020

The first step of the forest loss monitoring workflow is the use of an initial benchmark forest/non-forest mask (hereafter referred to as the forest mask), which accurately represents the forest area at the beginning of the change detection time window. The quality of the forest mask has a tremendous impact on the quality of the forest loss maps.

We compared various tree canopy cover maps detailed in the ATBD. We drew the following conclusions:

- The tree canopy cover 2010 from Hansen et al. (2013) can be updated to a 2017 forest mask by using the annual tree cover loss layer from GFW. However, it appeared that the quality of this map was much lower than the one from Potapov et al. (2019) (that is shown in Figure 4), partly because the 2010 map was produced using the Landsat 7 satellite data, whose the Scan Line Corrector in the Enhanced Thematic Mapper Plus (ETM+) instrument failed. A comparison between the two maps is shown in Figure 5,
- The accuracy of the forest/non-forest map from Shimada et al. (2014) was found to be too low,
- The Land use land cover maps 2017 from Trung et al. (2018), Duong et al. (2018) and Tung et al. (2016) have been derived in three parts (Northern, Central and Southern Vietnam) with two different methods, leading to spatial differences of quality. In addition, these maps covered Vietnam only,
- The spatial resolution of the fraction of green vegetation cover and the C3S global land cover was too coarse regarding the objectives of the SOFT project.

We finally selected the tree canopy cover map that has been produced in the frame of a joint project conducted by the GLAD laboratory from UMD and SERVIR-Mekong. The method used to derive the tree canopy cover map has been extensively described in Potapov et al. (2019). The obtained tree canopy cover (Figure 4) is defined as a proportion of canopy cover from woody vegetation taller than 5 m at 30 m pixel size from 2010 to 2017. Note that natural tree cover and tree plantation and agroforestry were not discriminated.

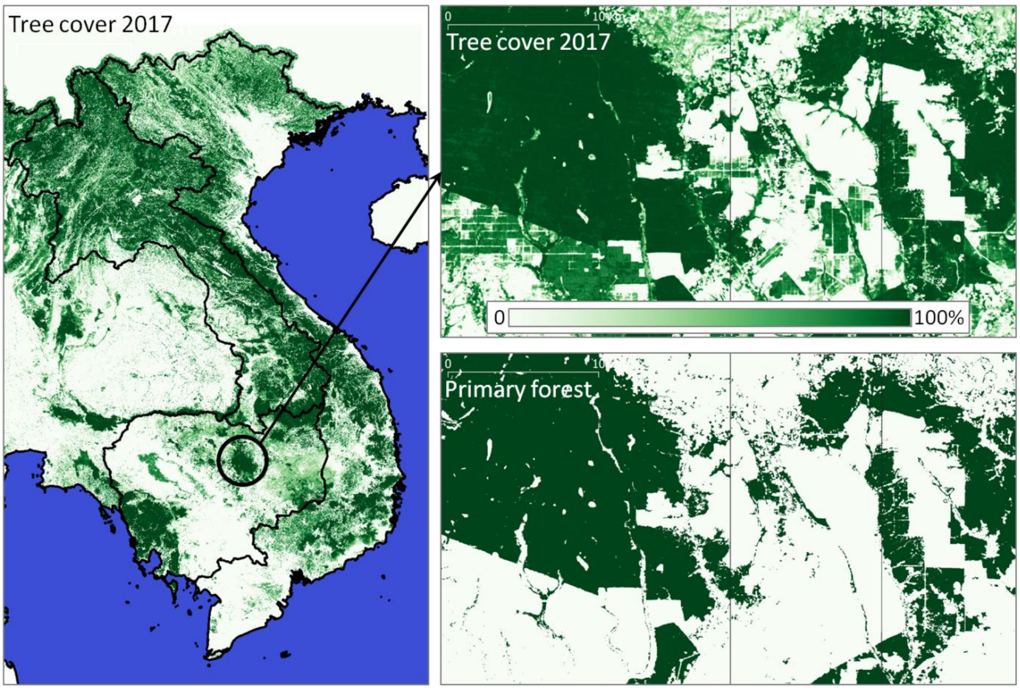

Figure 4. Tree canopy cover 2017 and primary forest extent at 30 m pixel size from Potapov et al. (2019)

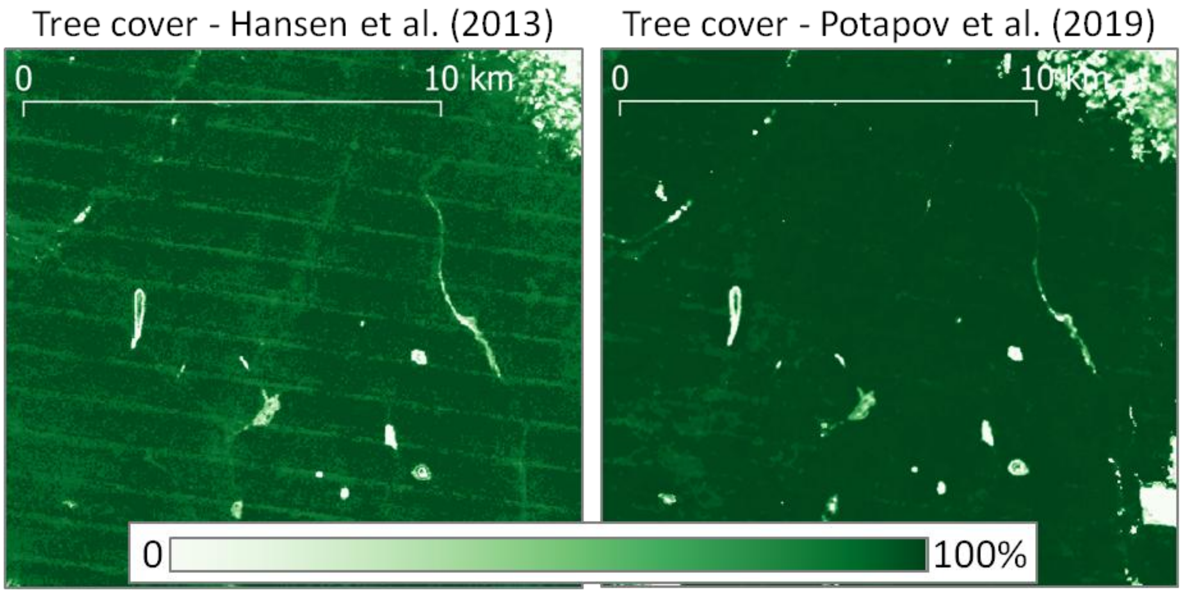

Figure 5. Comparison between the tree cover maps from Hansen et al. (2013) and Potapov et al. (2019). The map from Hansen is particularly affected by the failure of the Landsat -7 Scan Line Corrector in the Enhanced Thematic Mapper Plus (ETM+) instrument.

In addition to tree cover maps, we also used:

- Forest loss dataset from Hansen et al. (2013), from Hansen et al. (2016) and from JJ-FAST (Watanabe et al., 2017). Existing forest loss detection systems are useful in the SOFT project. These products were not considered here as benchmarks, but rather helped in the selection of study sites where forest losses are active and were compared with our forest loss maps.
- The last global forest canopy height map at 30 m resolution, which was developed recently through the integration of the Global Ecosystem Dynamics Investigation (GEDI) lidar forest structure measurements and Landsat analysis-ready data (ARD) time-series.
- Precipitations data. We analyzed rainfalls together with SAR backscatter using the Global Satellite Mapping of Precipitations (GSMaP) product (Kubota et al., 2020) to better understand the SAR backscatter behavior.

The above-mentioned dataset are fully described in the ATBD.

4.6 Analysis results in the frame of the PoC

Analyses of the Sentinel-1 backscatter signal over forest loss and intact forest areas of Vietnam, Cambodia and Laos were needed to adapt the forest loss detection method. Basic tools have therefore been developed to quickly analyze temporal images and backscatter profiles and for quick image vizualisation, which is useful to check the quality of the data before and after processing (problems related to geometric shifts and outliers in Sentinel-1 images). Figure 6 shows examples of temporal backscatter profiles over the tiles 48PWV, 48PYA and 48QXD. Temporal backscatter profiles consisted in profiles of backscatter and radar change ratio (RCR - Tanase et al., 2018) at VV and VH polarizations over reference data, and precipitations using the Global Satellite Mapping of Precipitations (GSMaP) product (Kubota et al., 2020). Temporal backscatter profiles allow to understand the backscatter temporal variations over plots with various characteristics, such as terrain slope and humidity due to rainfalls.

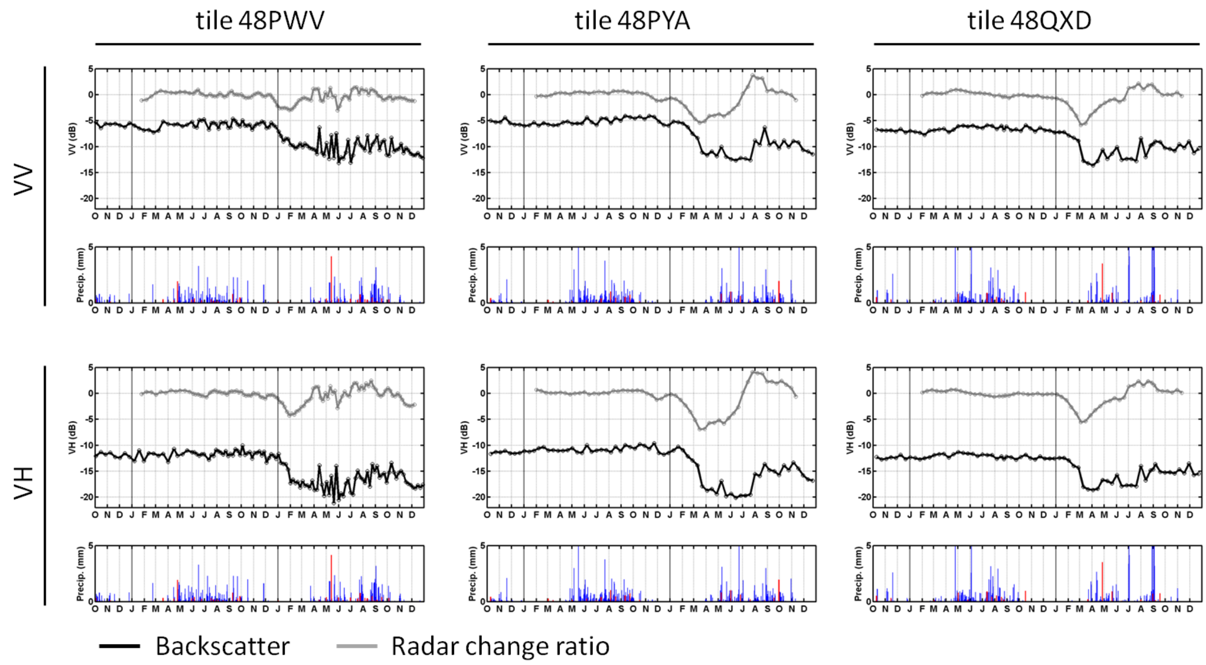

Figure 6. Backscatter γ^0_{VV} and radar change ratio (RCR) time series from October 2017 to end of 2019 for the tiles 48PWV, 48PYA and 48QXD. Precip means precipitations.

We also analysed the probability density function (PDF) and cumulative PDF of the minimum RCR indicator *min(RCR)* (Tanase et al., 2018, Bouvet et al., 2018) over the reference data of forest loss and intact forest areas, for each selected tile detailed in section 4.3, in ascending and descending modes separately. Figure 7 shows an example over the tile 48PVV. In Figure 7, the term «*shadows*» means that 25% of the pixels of each plot with the lowest *min(RCR)* values were used to draw the PDF.

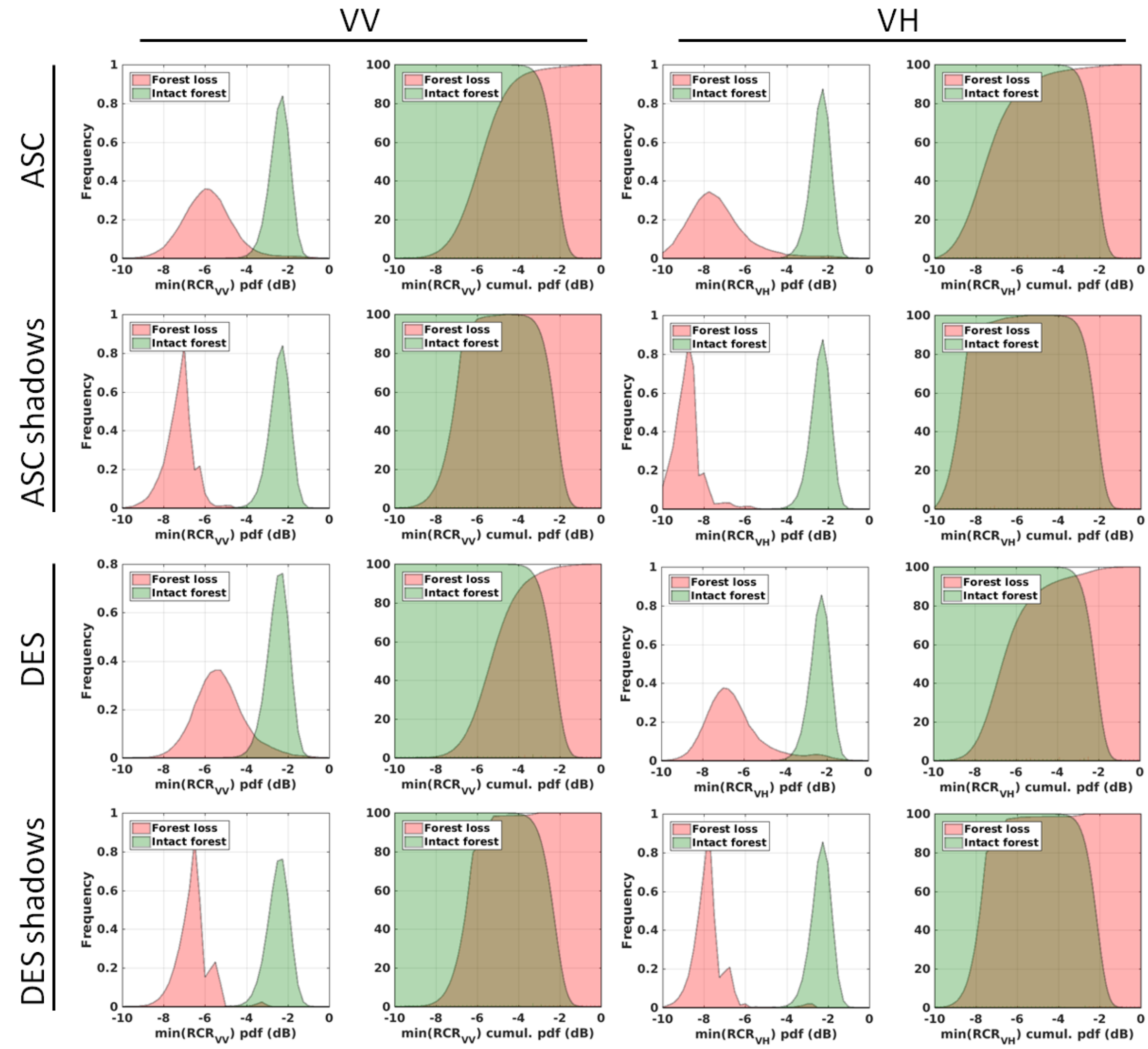

Figure 7. Probability density function (PDF) and cumulative PDF of the *min(RCR)* indicator at VV and VH polarization for reference data over the tile 48PVV in ascending (ASC) and descending (DES) modes. The term «*shadows*» means that 25% of the pixels of each plot with the lowest *min(RCR)* values were used to draw the PDF.

From these plots, we quantified the following indicators describing the separability of forest loss and intact forest reference data, with two different scenarii:

- **Scenario s1**: In this scenario, the true positive detection (TD) of the intact forest class is targetted to 95%, ensuring a trade-off between low false alarms rate and accurate forest loss detection. Note that TD is defined as true positive samples divided by the sum of true positive and false negative samples for a given *min(RCR)* threshold.
- **Scenario s2** : This scenario is more flexible. A range of indicator values is computed to correspond to various user needs, from detections with the highest possible certainty to avoid field teams being sent to sites at which deforestation events were falsely detected, to the most accurate map in term of producer and user accuracy.

In Table 5, the indicators described above were quantified for the tile 48PVV in ascending and descending modes. Regarding scenario 2, the range of values for each indicator in Table 5 are associated with the best 10 $E[TD_{FL} ,TD_{IF}]$-$s2$ values (FL and IF mean forest loss and intact forest respectively). We drew from these results the following conclusions :

- The separability between forest loss and intact forest reference data is obviously better when shadows are considered, as the pixels with the lowest *min(RCR)* values are selected in this case.
- Although results obtained at VV and VH polarizations are in general quite similar, results were systematically better at VH polarization as shown in the ATBD.
- The *min(RCR)* values were remarkably stable, ranging from -5.7 to -2.3 dB in general.

The indicators assessment for the other tiles of the PoC is detailed in the ATBD.

Table 5. Assessment of indicators describing the separability of forest loss and intact forest reference data over the tile 48PVV with two scenarii : **scenario s1** that is a trade-off between low false alarms rate and accurate forest loss detection and **scenario s2** corresponding to the most accurate map in term of producer and user accuracy. The ranges of values for each indicator of scenario 2 are associated with the best 10 ***E[TDFL ,TDIF]-s2*** values. The terms ***nb FL*** and ***nb IF*** refer to the number of pixels from the forest loss and intact forest reference dataset that were used for computing the indicators. The true positive detection ***TD*** is defined as true positive samples divided by the sum of true positive and false negative samples for a given ***min(RCR)*** threshold. The term **all** means that all available reference data were used, whereas the term **shad** means that 25% of the pixels of each plot with the lowest *min(RCR)* values were used.

						scenario 1		scenario 2			
				nb FL **x10^3**	***nb IF*** **x10^3**	***min(RCR)*** **s1 (db)**	**TD_{FL} s1 (%)**	***min(RCR)*** **s2 (db)**	**TD_{FL} s2 (%)**	**TD_{IF} s2 (%)**	**$E[TD_{FL} ,TD_{IF}]$ s2 (%)**
48PVV	**ASC 026**	**VV**	**all**	87	142	-3.1	97	-4.1 -3.2	92.1 96.7	99.8 95.8	96 97.2
			shad	22			100	-4.8 -3.9	99.7 100	100 99.7	99.8 100
		VH	**all**	87	142	-3	97.9	-4.3 -3.4	95.5 97.4	100 98.4	97.8 98.2
			shad	22			100	-5.5 -4.5	99.9 100	100 100	100 100
	DES 091	**VV**	**all**	87	142	-3.2	93.2	-4 -3.1	86 94.5	99.6 91.3	92.8 94.6
			shad	22			99.5	-5.1 -4.2	98.4 98.6	100 99.8	99.2 99.2
		VH	**all**	87	142	-3	95.7	-4.1 -3.2	92.2 95.2	99.9 96.9	96 96.7
			shad	22			99.2	-5 -4.1	98.5 98.6	100 99.9	99.2 99.3

4.7 Map resulting from the PoC

From the analysis above, we decided to restricted ourselves to the VH polarization to keep a consistent time series over the full date range. We applied the methodology fully described in the ATBD to the tiles selected in the frame of the PoC. We then discarded small outliers in the obtained maps by sieving and retained segments of more than 4 pixels, which correspond to a minimum mapping unit of 0.04 ha. The resulting forest loss map is shown in Figure 8, where the indicated numbers correspond to specific areas shown in Figure 9. Figure 9 shows forest loss in plantations (subfigure 9 in Figure 9) versus natural forest (e.g. subfigures 5 and 6), logging roads (subfigure 7), and small disturbed areas (subfigure 3) versus large disturbed areas (subfigure 6). Figure 9 also highlights the high rate of good detection (forest loss reference data in red) and low rate of false alarms (intact reference data in green).

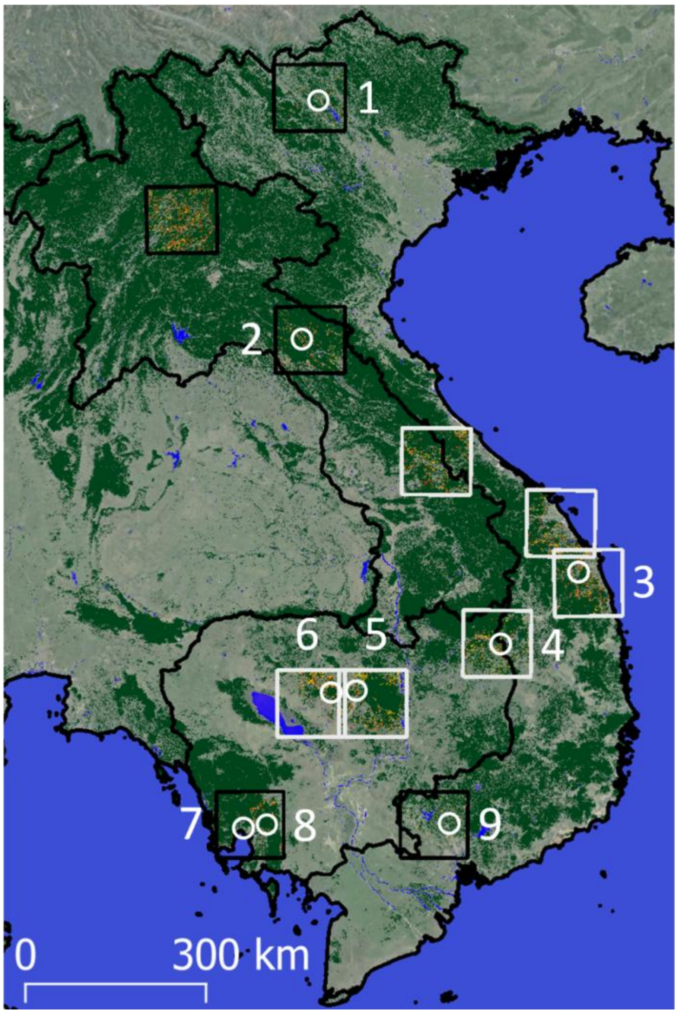

Figure 8. Forest loss detection results over the tiles selected in the frame of the PoC. Forest areas from Potapov et al. (2019) are in dark green and the background image is from Google Earth. The indicated numbers correspond to specific areas presented in Figure 9.

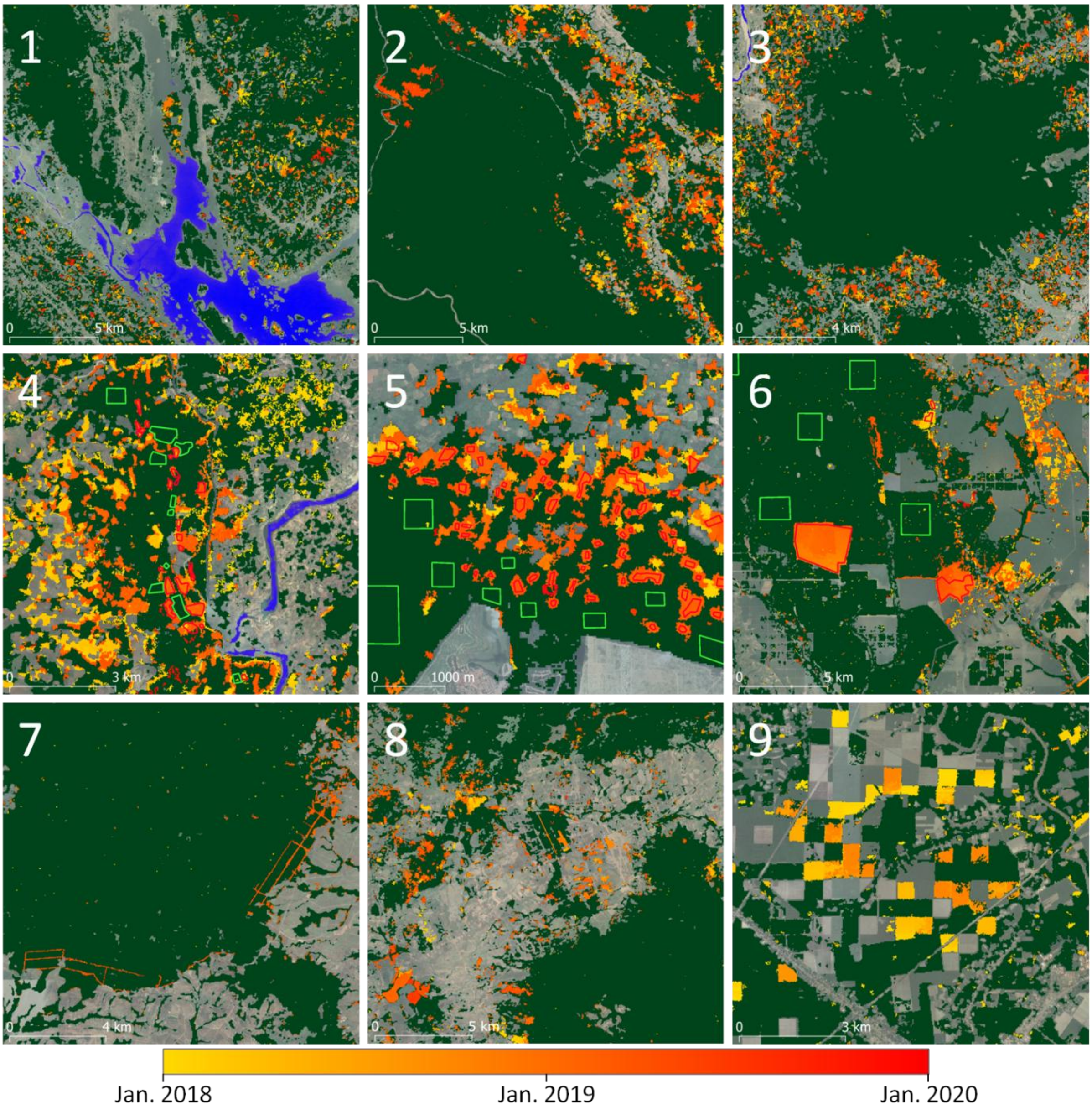

Figure 9. Visual comparison of forest loss detection results, highlighting the various sizes and distributions of disturbed areas. Intact forest and forest loss reference data are drawn in green and red respectively. Forest areas from Potapov et al. (2019) are in dark green and the background image is from Google Earth.

We computed confusion matrices (Table 6) for the tiles 49PBS and 48PZC, where reference data were selected and where terrain relief is the steepest. Producer, user and overall acuracy were found to be higher than 94% and kappa index higher than 0.96. We noticed a slight over-estimation of detected forest losses (UA of 94% for the two tiles). However, these results showed that accurate forest loss detection is possible, even over hilly or mountainous areas.

Table 6. Assessment (pixel counting) of the forest loss detection method accuracy for the tile 49PBS (left) and 48PZC (right). Columns show the forest loss (FL) and intact forest (IF) as determined by the detection method, whereas rows indicate the reference data. PA, UA and OA are in % and stand for producer, user and overall acuracy, k stands for kappa index.

	FL	**IF**	UA
FL	25 315	1 380	94.8
IF	0	418 231	100
PA	100	99.7	
OA	99.7		
k	0.97		

	FL	**IF**	UA
FL	12 561	730	94.5
IF	211	71 487	99.7
PA	98.3	99	
OA	98.9		
k	0.96		

5 ACTIVITIES PERFORMED AND RESULTS: WP 300

In the frame of WP 300, we mainly optimized, installed and ran the scripts (in Python) onto the high performance computing (HPC) cluster of the CNES.

The main technical challenge was the processing of the large amount of available Sentinel-1 data (see Figure 10), with 37 and 34 frames of Sentinel-1 data in ascending and descending geometry respectively, to cover the whole study area. Given the small duration of the project and the amount of data to be processed, we started to work on this WP from the beginning of the project.

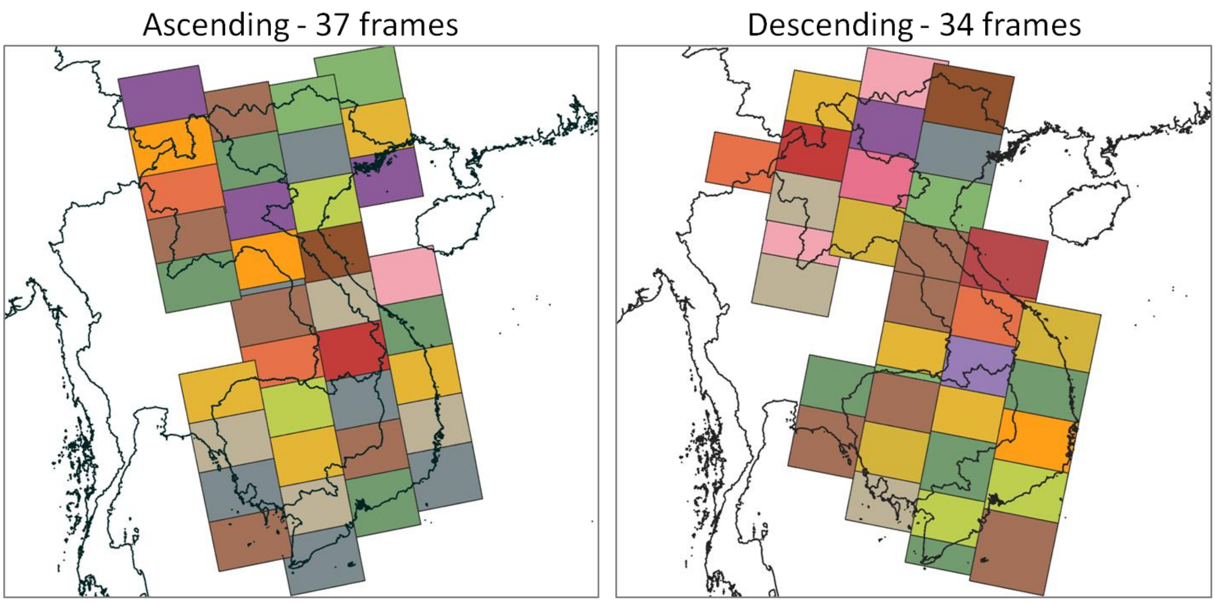

Figure 10. Number and distribution of Sentinel-1 frames in ascending and descending modes over Vietnam, Cambodia and Laos.

In the frame of the extension of the GeoRice project funded by ESA (Contract Change Notice number 1 of the ESA Contract 4000113388/15/I-NB) and conducted by CESBIO and GlobEO, a part of Sentinel-

1 data used in the SOFT project, over Vietnam, Cambodia and Laos was already processed at the beginning of the SOFT project and made available in the CEOS analysis ready data (ARD) format in sigma naught. To complete the processing specific to the SOFT project (i.e. to forest monitoring), we first processed and standardized all the data needed to convert sigmal naught Sentinel-1 backscatter from the GeoRice project to topographic-corrected gamma naught, i.e., terrain slope and aspect angles, and local incidence angles. We downloaded and fully processed the Sentinel-1 dataset in ascending mode from 2018 to 2021 and in descending mode in 2020 (not processed in the frame of the GeoRice project) and converted sigmal naught Sentinel-1 backscatter to topographic-corrected gamma naught over selected test sites. We then filtered in NRT mode the Sentinel-1 images. To do so, each new acquired image was filtered using previously acquired images, instead of filtering the whole stack of images.

We could handle efficiently the large amount of Sentinel-1 data available using the pre-processing chain developed at CESBIO, detailed in the ATBD. The chain is highly scalable (multithreading / multiprocessor), which made it easy to install onto the high performance computing (HPC) CNES cluster in May 2020. After the installation of the codes, we performed tests of the various scripts (NRT speckle filtering, detection of forest loss, post-processing). We also fixed some problems related to data management, e.g. the large amount of Sentinel-1 data by compressing input and output data and removing input data on-the-fly when not necessary anymore in the detection algorithm.

Then, the processing of the whole study area has been achieved. We mosaicked the resulting maps, checked their quality and manually corrected outliers. Outliers were found to be rare as the forest loss detection method is not applied over areas with potential false alarms, i.e. with backscatter varying in time (such as water areas, bare soils, mangroves and non forest areas in general). Nevertheless, some tiles had to be reprocessed due to flaws in the acquisition of the Sentinel-1 data, leading for example to geometric inconsistencies.

The final forest loss map over Vietnam, Laos and Cambodia from 2018 to 2021, is shown in Figure 11. The map provides clear hints of the spatial and temporal distribution of forest losses. For example, Figure 12 shows the difference between high forest losses currently happening in Northern Laos versus low forest losses in Northern Vietnam, although the whole Northern mountainous region is covered by similar forest types.

Specific areas of the whole forest loss map are shown in Figure 13. Figure 13 shows forest loss in various environments and forest types, from North to South of the study area. It is important to note that the method provided accurate results whatever the topography, as emphasized in the ATBD following the results of the PoC.

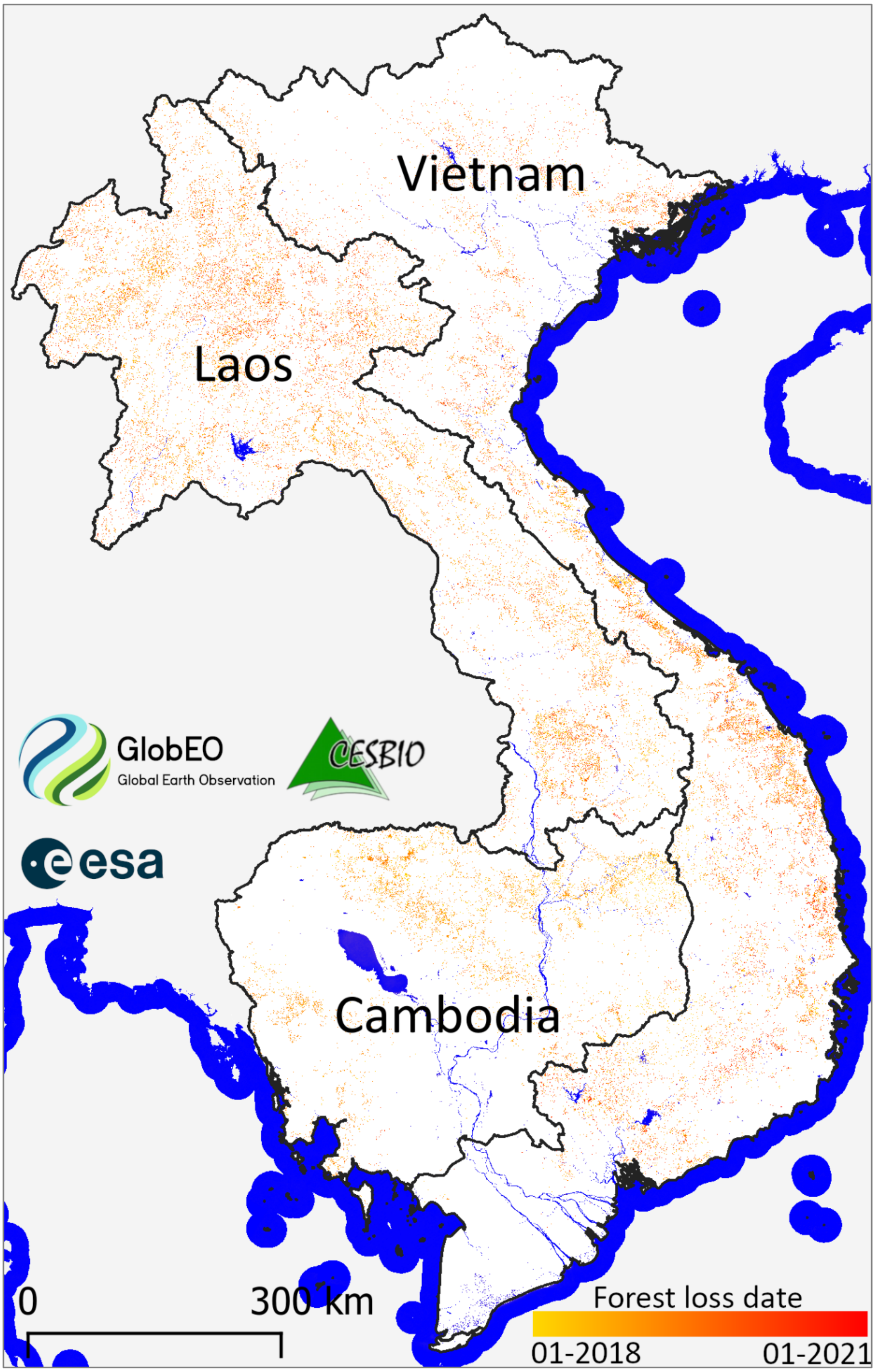

Figure 11. Forest disturbances map using Sentinel-1 data in Vietnam, Laos and Cambodia from the end of 2017 to the beginning of 2021.

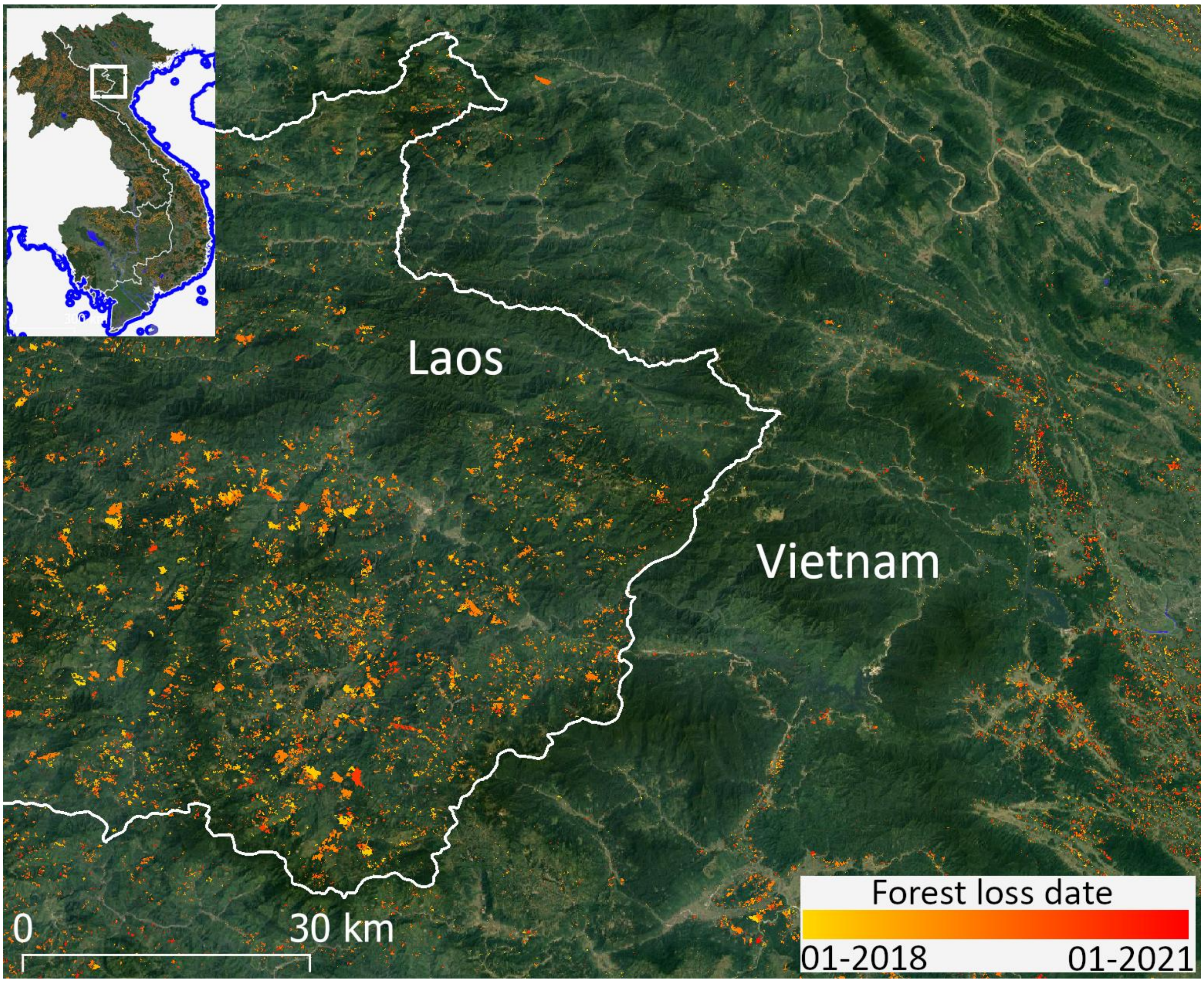

Figure 12. Forest disturbances map using Sentinel-1 data at the border between Laos and Vietnam, from the end of 2017 to the beginning of 2021. The background image is from Google Earth. The map evidences high forest losses currently happening in Northern Laos versus low forest losses in Northern Vietnam.

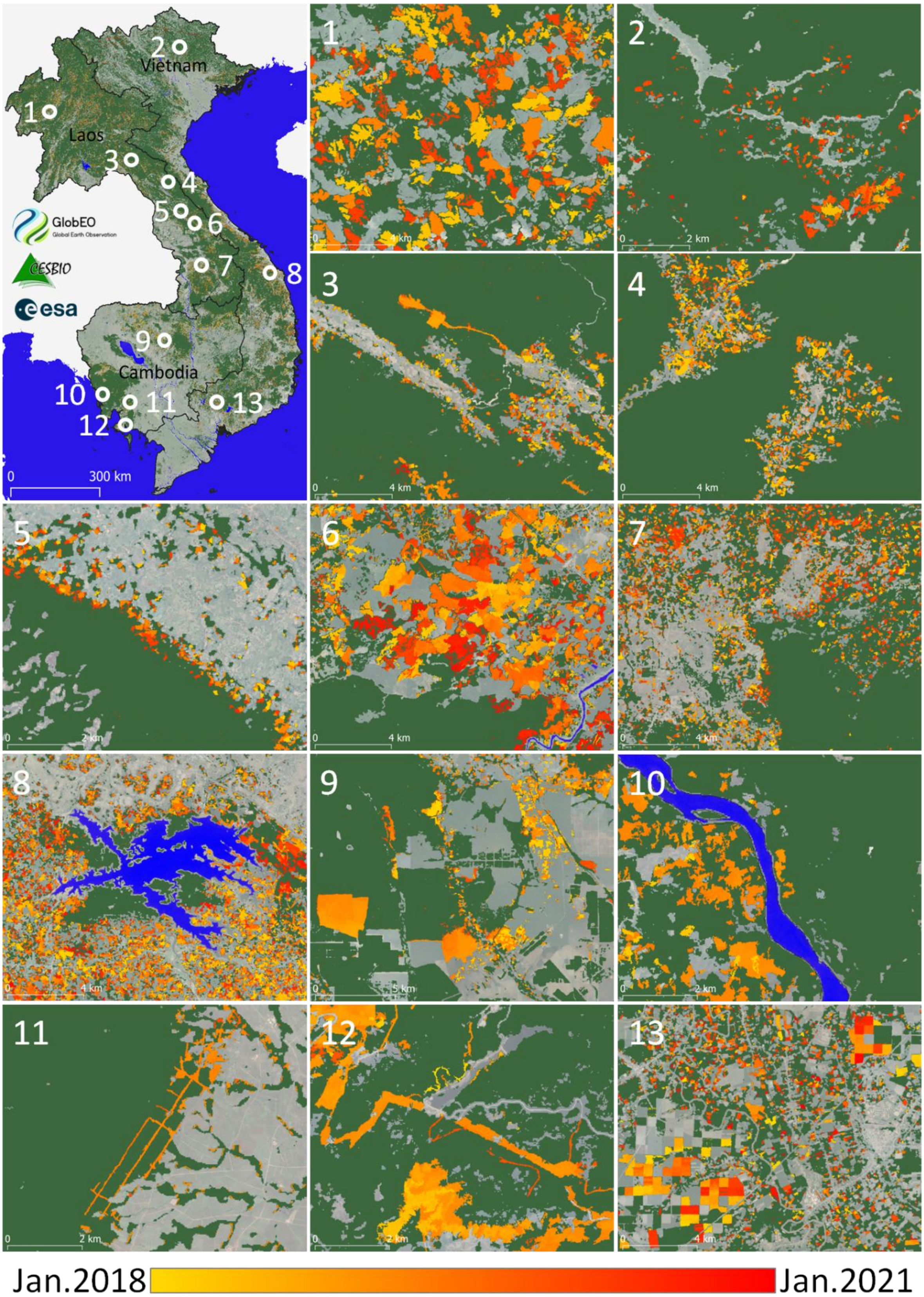

Figure 13. Visual comparison of forest loss detection results, highlighting the various sizes and distributions of disturbed areas. Forest areas from Potapov et al. (2019) are in dark green and the background image is from Google Earth.

We also compared the forest loss surface areas obtained from our method with the results from GFW and GLAD. Although we do not consider the maps of GFW and GLAD as a benchmark and although the use of Sentinel-1 is basically much more relevant in term of timely detection of forest losses, we quantitatively compared the statistics per year and country (Table 7) and qualitatively compared both maps (Figure 14). Note that at the time of the writting, the GFW maps were not available for the year 2020. We also wrote to the GLAD team to ask for the GLAD 2018 alerts (that are not available anymore on line), but did not receive any answer. The results from this study and from GFW are remarkably similar, the largest difference (23%) being found for Laos in 2019. This result highlights the fact that our detection system can be used as an alert system (fast detection from sentinel-1 data) and as an annual detection system similar to GFW, used for example to compute national statistics. As expected, the GLAD alerts allowed to detect much less forest loss areas, with notable time delays (see Ballère et al., 2021 for a detailed analysis on this topic).

Table 7. Surface areas per year and country in hectare, from this study, Global Forest Watch (Hansen et al., 2013) and GLAD (Hansen et al., 2016).

	This study	**GFW (Hansen et al., 2013)**	**GLAD (Hansen et al., 2016)**
Vietnam 2018	345 121	422 300	-
Vietnam 2019	445 977	421 910	83 361
Vietnam 2020	333 655	-	-
Cambodia 2018	200 400	180 970	-
Cambodia 2019	281 335	236 780	119 042
Laos 2018	327 152	400 290	-
Laos 2019	648 089	498 830	153 187
Laos 2020	292 383	-	-

We performed visual comparisons between the maps resulting from our study and from GFW. The example in Figure 14 (Up) illustrates the fact that in many areas, the results from both methods are rather similar. However, the exemple in Figure 14 (Bottom) emphasizes a phenomenon that is common in the resulting maps : only the edges of the disturbed areas are detected in the GFW maps, contrary to the maps from our method in which the disturbed areas are accurately detected.

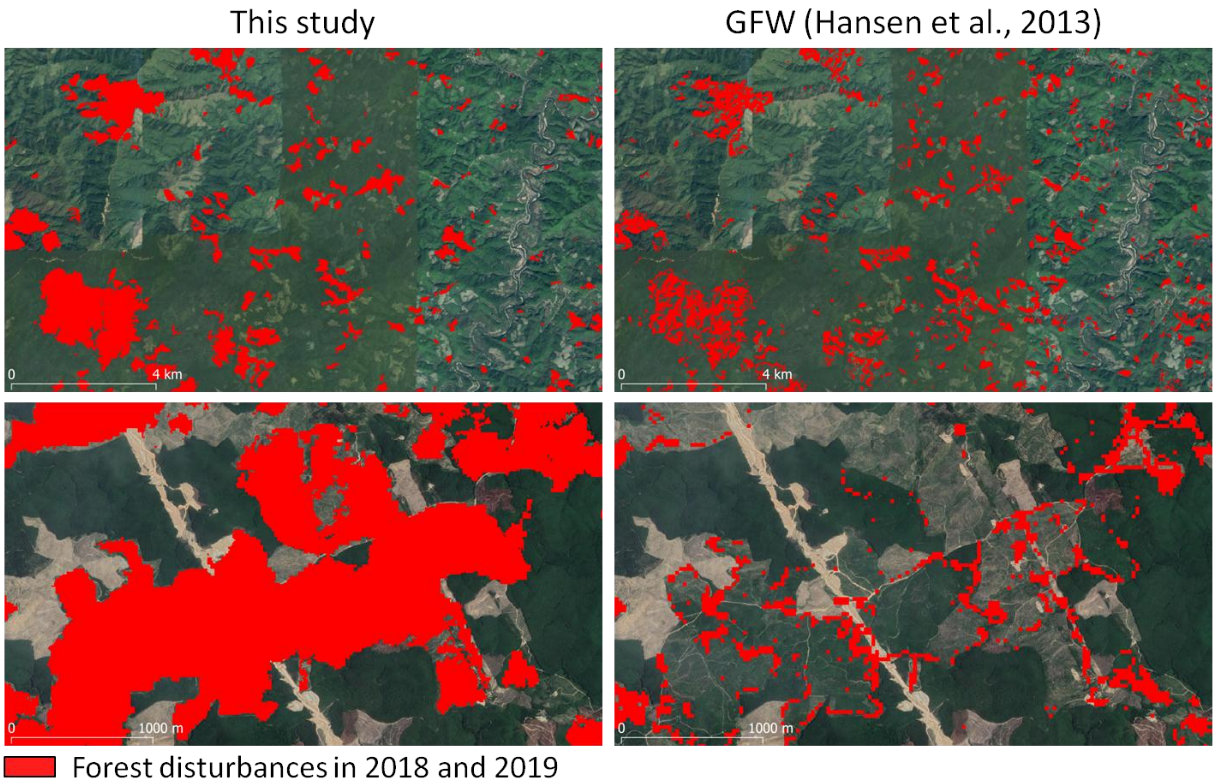

Figure 14. Visual comparison between the forest disturbances maps from this study (Left) and from Global Forest Watch (Right). The two areas are centred on 102.75°N and 20.48°E in Laos (Up) and 107.21°N and 16.61°E in Vietnam (Bottom). The background image is from Google Earth.

6 ACTIVITIES PERFORMED AND RESULTS: WP 400

The validation framework is primarily based on the good practices recommended by Olofsson et al. (2014 and 2020).

In the frame of the SOFT project, we chose as sampling design a stratification with stratas defined by the map classes, mainly to improve the precision of the accuracy and area estimates. The stratified design satisfies the basic accuracy assessment objectives and most of the desirable design criteria. We selected a buffer stratum in addition to an intact forest stratum and a forest disturbances stratum, for the reasons detailed in the validation report and as recommanded by Olofsson et al. (2020).

We specified a target standard error for overall accuracy of 0.01 and supposed that user's accuracies of the change class is 0.70 for forest disturbances and 0.90 for intact forest. The resulting sample size is therefore n=803 in total, which we have rounded up to 1 000 samples.

We then assessed the allocation of the sample to strata so that the sample size allocation results in precise estimates of accuracy and area. We followed Olofsson's recommendations and allocated a sample size of 100 for the forest disturbance stratum, and then allocated the remainder of the samples to the intact forest classes, i.e. 200 in the buffer areas around detected disturbances, and 700 in intact forest outside of these buffers. Figure 15 shows the location of the 1 000 samples in the study area.

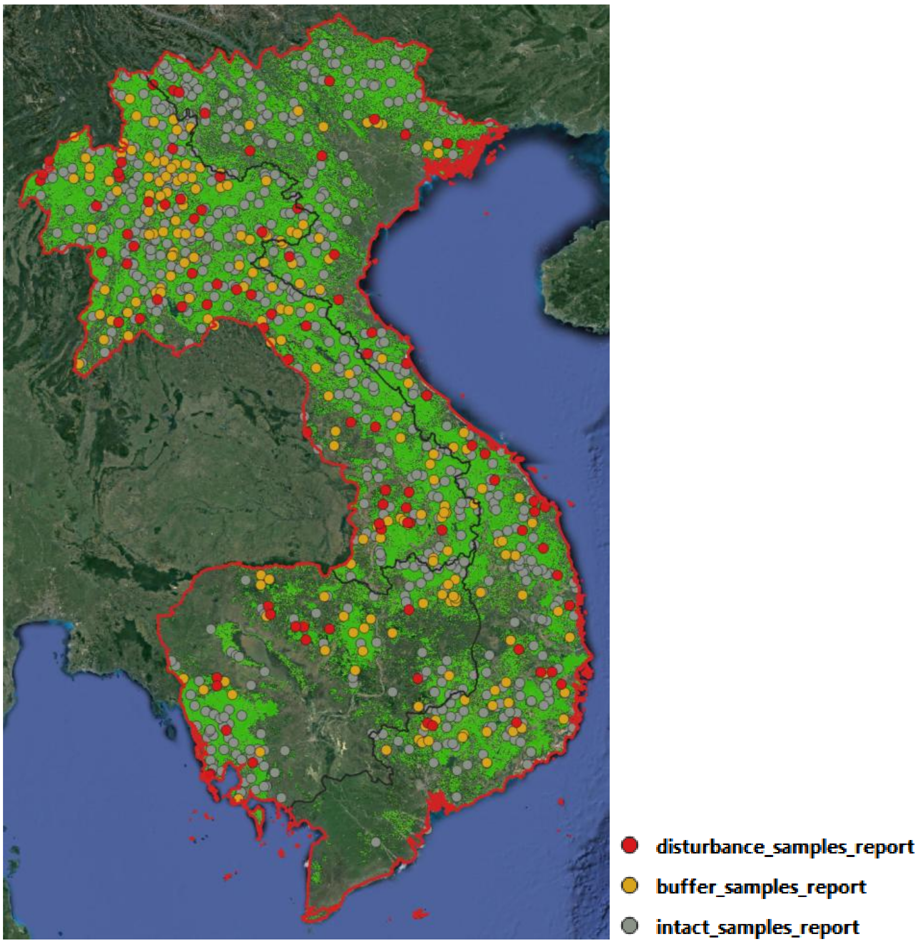

Figure 15. Location of the 100 disturbance samples, 200 buffer samples (intact forest around disturbance) and 700 intact forest samples used for the validation. Light green areas represent the baseline forest map.

Both high- and very high spatial resolution (<10 m and <1 m respectively) satellite data were viable candidates for reference data. We used when possible freely accessible very high spatial resolution imagery online through Google Earth™ (Google, 2011), which presents low cost interpretation options. Google Earth images are actually a relatively relevant source of validation data for remote sensing studies. When Google Earth images were not available at the relevant dates, we instead accessed Planet's very high-resolution analysis-ready mosaics as reference data. Through Norway's International Climate and Forests Initiative, these pan-tropical 4.8 m resolution mosaics were recently released in order to help reduce the loss of tropical forests, amongst others.

The resulting confusion matrix presented in terms of the sample counts is displayed in Table 8, and the confusion matrix populated by estimated proportions of area, used to report accuracy results is shown in Table 9.

Table 8. Error matrix of sample counts

		Reference				
		Disturbances	**Intact**	Total	$A_{m,i}$ (km²)	W_i
Map	**Disturbances**	96	5	101	22 222	5.84%
	Intact buffer	3	194	197	70 667	18.58%
	Intact	3	693	696	287 462	75.58%
	Total	102	892	994	380 351	100%

Table 9. Error matrix in Table 8 populated by estimated proportions of area, used to report accuracy results

		Reference			
		Disturbances	**Intact**	Total (W_i)	$A_{m,i}$ (km²)
Map	**Disturbances**	5.55%	0.29%	5.84%	22 222
	Intact buffer	0.28%	18.30%	18.58%	70 667
	Intact	0.33%	75.25%	75.58%	287 462
	Total	6.16%	93.84%	100%	380 351

We then estimated from the confusion matrix in Table 9 user's accuracy, producer's accuracy and overall accuracy. Variances for these accuracy measures are estimated using Eqs. (5)–(7) from Olofsson et al. (2014):

- The estimated **user's accuracy** (±95% confidence interval) is **0.950** ± 0.043 for forest disturbances and **0.993** ± 0.005 for intact forest (including buffer areas around disturbance).
- The estimated **producer's accuracy** is **0.898** ± 0.061 for forest disturbances and **0.997** ± 0.043 for intact forest.
- The estimated **overall accuracy** is **0.991** ± 0.006.

We also estimated area proportions from the confusion matrix in Table 9. The row totals of the confusion matrix give the mapped area proportions W_i while the column totals give the estimated area proportions according to the reference data. Multiplying the latter by the total mapped area gives the stratified area estimate of each class according to the reference data. For example, the estimated area of 2018 and 2019 deforestation according to the reference data is $\hat{A}_{dis}$=$\hat{p}_{.dis} \times A_{tot} = 0.0616 \times 380\ 351$ km² $= 23\ 437$ km². The mapped area of deforestation $A_{m,1}$ of 22 222 km² was thus underestimated by 1 215 km².

The final step is to estimate a confidence interval for the area of each class. From Eq. (10) in Olofsson et al (2014), $S(\hat{p}_{.dis}) = 0.0029$ and the standard error for the estimated area of forest loss is $S(\hat{A}_{dis})$=$S(\hat{p}_{.dis}) \times A_{tot} = 0.0029 \times 380\ 351$ km² $= 1\ 092$ km². The margin of error of the confidence interval is 1.96 × 1 092 = 2 140 km². We have thus estimated the area of deforestation with a 95% confidence interval: 23 437 ± 2 140 km².

7 REFERENCES

Ballère, M., Bouvet, A., Mermoz, S., Le Toan, T., Koleck, T., Bedeau, C., ... & Lardeux, C. (2021). SAR data for tropical forest disturbance alerts in French Guiana: Benefit over optical imagery. Remote Sensing of Environment, 252, 112159.

Bouvet, A., Mermoz, S., Ballère, M., Koleck, T., & Le Toan, T. (2018). Use of the SAR shadowing effect for deforestation detection with Sentinel-1 time series. Remote Sensing, 10(8), 1250.

Diniz, C. G., De Almeida Souza, A. A., Santos, D. C., Dias, M. C., da Luz, N. C., de Moraes, D. R. V., ... & Adami, M. (2015). DETER-B: The new Amazon near real-time deforestation detection system. IEEE Journal of Selected Topics in Applied Earth Observations and Remote Sensing, 8(7), 3619-3628.

Doblas, J., Carneiro, A., Shimabukuro, Y., Sant'Anna, S., Aragão, L., & Pereira, F. R. S. (2020). Stabilization of sentinel-1 SAR time-series using climate and forest structure data for early tropical deforestation detection. ISPRS Annals of the Photogrammetry, Remote Sensing and Spatial Information Sciences, 3, 89-96.

Duong, P. C., Trung, T. H., Nasahara, K. N., & Tadono, T. (2018). JAXA High-Resolution Land Use/Land Cover Map for Central Vietnam in 2007 and 2017. Remote Sensing, 10(9), 1406.

FAO. Global Forest Resources Assessment; Technical Report; Food and Agriculture Association of the United-States: Rome, Italy, 2020.

Finer, M., Novoa, S., Weisse, M.J., Petersen, R., Mascaro, J., Souto, T., Stearns, F., Martinez, R.G., 2018. Combating deforestation: From satellite to intervention. Science 360, 1303–1305. https://doi.org/10.1126/science.aat1203

Google, C. (2010). Google earth. Accessed on 2020 and 2021.

Hansen, M. C., Potapov, P. V., Moore, R., Hancher, M., Turubanova, S. A., Tyukavina, A., ... & Kommareddy, A. (2013). High-resolution global maps of 21st-century forest cover change. Science, 342(6160), 850-853.

Hansen, M. C., Krylov, A., Tyukavina, A., Potapov, P. V., Turubanova, S., Zutta, B., ... & Moore, R. (2016). Humid tropical forest disturbance alerts using Landsat data. Environmental Research Letters, 11(3), 034008.

Harris, N., E. Goldman and S. Gibbes. "Spatial Database of Planted Trees (SDPT) Version 1.0." Accessed through Global Forest Watch on 10/04/2020. www.globalforestwatch.org.

Houghton, R.A., Nassikas, A.A., 2017. Global and regional fluxes of carbon from land use and land cover change 1850-2015: Carbon Emissions From Land Use. Glob. Biogeochem. Cycles 31, 456–472. https://doi.org/10.1002/2016GB005546.

Kubota, T., K. Aonashi, T. Ushio, S. Shige, Y. N. Takayabu, M. Kachi, Y. Arai, T. Tashima, T. Masaki, N. Kawamoto, T. Mega, M. K. Yamamoto, A. Hamada, M. Yamaji, G. Liu and R. Oki 2020: Global Satellite Mapping of Precipitation (GSMaP) products in the GPM era, Satellite precipitation measurement, Springer.

Lohberger, S., Stängel, M., Atwood, E.C., Siegert, F., 2018. Spatial evaluation of Indonesia's 2015 fire-affected area and estimated carbon emissions using Sentinel-1. Glob. Change Biol. 24, 644–654. https://doi.org/10.1111/gcb.1384.

Mermoz, S., & Le Toan, T. (2016). Forest disturbances and regrowth assessment using ALOS PALSAR data from 2007 to 2010 in Vietnam, Cambodia and Lao PDR. Remote Sensing, 8(3), 217.

Olofsson, P., Foody, G. M., Herold, M., Stehman, S. V., Woodcock, C. E., & Wulder, M. A. (2014). Good practices for estimating area and assessing accuracy of land change. Remote Sensing of Environment, 148, 42-57.

Olofsson, P., Arévalo, P., Espejo, A. B., Green, C., Lindquist, E., McRoberts, R. E., & Sanz, M. J. (2020). Mitigating the effects of omission errors on area and area change estimates. Remote Sensing of Environment, 236, 111492.

Potapov, P., Li, X., Hernandez-Serna, A., Tyukavina, A., Hansen, M. C., Kommareddy, A., ... & Hofton, M. (2021). Mapping global forest canopy height through integration of GEDI and Landsat data. Remote Sensing of Environment, 253, 112165.

Potapov, P., Siddiqui, B. N., Iqbal, Z., Aziz, T., Zzaman, B., Islam, A., ... & Hansen, M. C. (2017). Comprehensive monitoring of Bangladesh tree cover inside and outside of forests, 2000–2014. Environmental Research Letters, 12(10), 104015.

Reiche, J., Mullissa, A., Slagter, B., Gou, Y., Tsendbazar, N. E., Odongo-Braun, C., ... & Herold, M. (2021). Forest disturbance alerts for the Congo Basin using Sentinel-1. Environmental Research Letters, 16(2), 024005.

Reiche, J., Verhoeven, R., Verbesselt, J., Hamunyela, E., Wielaard, N., & Herold, M. (2018). Characterizing tropical forest cover loss using dense sentinel-1 data and active fire alerts. Remote Sensing, 10(5), 777.

Reiche, J., Lucas, R., Mitchell, A.L., Verbesselt, J., Hoekman, D.H., Haarpaintner, J., Kellndorfer, J.M., Rosenqvist, A., Lehmann, E.A., Woodcock, C.E., Seifert, F.M., Herold, M., 2016. Combining satellite data for better tropical forest monitoring. Nat. Clim. Change 6, 120–122. https://doi.org/10.1038/nclimate2919.

Reymondin, L., Jarvis, A., Perez-Uribe, A., Touval, J., Argote, K., Coca, A., Rebetez, J., Guevara, E., Mulligan, M., 2012. Terra-i : A methodology for near real-time monitoring of habitat change at continental scales using MODIS-NDVI and TRMM.

Shimada, M., Itoh, T., Motooka, T., Watanabe, M., Shiraishi, T., Thapa, R., & Lucas, R. (2014). New global forest/non-forest maps from ALOS PALSAR data (2007–2010). Remote Sensing of environment, 155, 13-31.

Stehman, S. V., Olofsson, P., Woodcock, C. E., Herold, M., & Friedl, M. A. (2012). A global land-cover validation data set, II: Augmenting a stratified sampling design to estimate accuracy by region and land-cover class. International Journal of Remote Sensing, 33(22), 6975-6993.

Tanase, M. A., Aponte, C., Mermoz, S., Bouvet, A., Le Toan, T., & Heurich, M. (2018). Detection of windthrows and insect outbreaks by L-band SAR: A case study in the Bavarian Forest National Park. Remote Sensing of Environment, 209, 700-711.

Trung, T.H. Land Cover Change Mapping in Southern Vietnam Using Multi-temporal High resolution Satellite Remote Sensing Data, Master’s thesis, University of Tsukuba, 2018.

Tung, T. Analysis of Land Cover Change in Northern Vietnam Using High Resolution Remote Sensing Data, Hoang, Master’s thesis, University of Tsukuba, 2016.

Watanabe, M., Koyama, C., Hayashi, M., Kaneko, Y., Shimada, M., 2017. Development of early-stage deforestation detection algorithm (advanced) with PALSAR-2/ScanSAR for JICA-JAXA program (JJ-FAST). IEEE, pp. 2446–2449. https://doi.org/10.1109/IGARSS.2017.8127487.

Wheeler, D., Hammer, D., Kraft, R., Steelr, A., 2014. Satellite-based forest clearing detection in the brazilian amazon: FORMA, DETER, and PRODES. World Resources Institute: Washington, DC, USA.

World Wildlife Fund. (2013). Ecosystems in the Greater Mekong: Past trends, current status, possible futures.